ROYAL SOCIETY OPEN SCIENCE

Non-invasive biophysical measurement of travelling waves in the insect inner ear

Journal:	*Royal Society Open Science*
Manuscript ID	RSOS-170171.R1
Article Type:	Research
Date Submitted by the Author:	31-Mar-2017
Complete List of Authors:	Sarria-S, Fabio; University of Lincoln, School of Life Sciences Chivers, Benedict; University of Lincoln, School of Life Sciences Soulsbury, Carl; University of Lincoln, School of Life Sciences Montealegre-Z, Fernando; University of Lincoln, School of Life Sciences
Subject:	biophysics < BIOLOGY, neuroscience < BIOLOGY, physiology < BIOLOGY
Keywords:	Travelling wave, cochlea, hearing, laser vibrometry, spectrophotometry
Subject Category:	Biology (whole organism)

Non-invasive biophysical measurement of travelling waves in the insect inner ear

Short title: non-invasive measurement of an inner ear

Author affiliations:

Fabio A. Sarria-S[1]

Benedict D. Chivers[1]

Carl D. Soulsbury[1]

Fernando Montealegre-Z[1]

1 School of Life Sciences, Joseph Banks Laboratories, University of Lincoln, Lincoln, LN6 7DL, United Kingdom

Keywords:

Travelling wave, cochlea, tonotopy, hearing, laser vibrometry, katydid

Author for correspondence:

Fernando Montealegre-Z,

e-mail: fmontealegrez@lincoln.ac.uk

Abstract

Frequency analysis in the mammalian cochlea depends on the propagation of frequency information in the form of a travelling wave (TW) across tonotopically arranged auditory sensilla. TWs have been directly observed in the basilar papilla of birds and the ears of bush-crickets (Insecta: Orthoptera) and have also been indirectly inferred in the hearing organs of some reptiles and frogs. Existing experimental approaches to measure TW function in tetrapods and bush-crickets are inherently invasive, compromising the fine-scale mechanics of each system. Located in the forelegs, the bush-cricket ear exhibits outer, middle and inner components; the inner ear containing tonotopically arranged auditory sensilla within a fluid-filled cavity, and externally protected by the leg cuticle. Here, we report bush-crickets with transparent ear cuticles as potential model species for direct, non-invasive measuring of TWs and tonotopy. Using laser Doppler vibrometry and spectroscopy, we show that increased transmittance of light through the ear cuticle allows for effective non-invasive measurements of TWs and frequency mapping. More transparent cuticles allow several properties of TWs to be precisely recovered and measured in vivo from intact specimens. Our approach provides an innovative, non-invasive alternative to measure the natural motion of the sensillia-bearing surface embedded in the intact inner ear fluid.

1. Introduction

Among vertebrates, mammals and birds exhibit an elaborate hearing system, in which auditory perception relies on mechanical and neurophysiological processes occurring in the fluid-filled cochlea [1]. Frequency discrimination occurs in the cochlea, a coiled, fluid filled structure of bone located inside the skull. Sound is decomposed in a spatial frequency map characterised as tonotopy. This is supported by an oscillatory motion travelling along the length of the basilar membrane, a structure inside the cochlea, which bears the stereocilia (sensory cells). This travelling wave (TW) propagates inside the cochlea and generates an amplitude maxima response at frequency-dependent locations [2]. The mechanical displacement at resonant points stimulates the sensory receptor cells initiating a neural response.

First used to describe the motion of the basilar membrane in the cochleae of human cadavers [3], passive TWs are viewed today as the substratum for active cochlear amplification in mammals [1, 4]. Phenomena analogous to TW have been directly observed in the basilar papilla of birds (Aves) [5] and the ears of bush-crickets (Insecta) [6, 7], and have also been inferred, via the timing of responses of auditory-nerve fibres, in the hearing organs of some reptiles and frogs [8, 9]. In vertebrates, the structure and location of the inner ear make it almost impossible to access without altering its integrity [1, 7, 10]. Measurements *in vivo* have only been done through small openings in the *scala tympani* or other isolated places [10, 11, 12]. Indirectly, the spatial frequency response on the basilar membrane (BM) has also been inferred through computational models, or estimated from auditory afferent nerve fibres at selected points [13, 14]. Hitherto, there lacks an easy, non-invasive approach to directly access the complex auditory processes occurring with the cochlea

Bush-crickets (Orthoptera: Tettigoniidae) are insects that exploit acoustic signals to interact with their conspecifics [15-17]. Both males and females detect acoustic signals using paired tympanal organs located on their forelegs (figure 1*a*), just below the femoro-tibial joint [18-20]. The tympanal organ is backed by an acoustic tracheal tube connecting the ear with the thoracic spiracle [21]. Just at the tympanal region the trachea splits in two forming a fold with a triangular and slightly curved/convex surface, which contains a collection of mechanoreceptors aligned in a row forming a crest, known as the *crista acustica* (CA). Bush-crickets exhibit a highly-sophisticated hearing system that includes an outer, middle, and an inner ear, which exhibit basic auditory processes analogous to the mammalian system [6]. Although a large number of questions remain to be answered before the two ears can be seen as equivalent, both systems can be compared in a broad sense. The bush-cricket inner ear formed by the CA and auditory vesicle (AV), allows effective frequency discrimination through tonotopy and TWs [22-24]. Similar to the mammalian basilar membrane in the cochlea, sound-induced TWs originate at the narrow, distal, high-frequency end of the CA, and propagate towards the wide, low-frequency, proximal region of the same structure [6, 7]. This mechanical motion enhances the tonotopic response at a specific resonant location where the TW reaches its maximum displacement [25].

Innovative approaches and organisms with easy-to-access inner ears could provide alternative solutions to advance our understanding of complex auditory processes. Bush-crickets provide an ideal model, having ears which lays beneath the leg cuticle allowing researchers to measure TWs and tonotopy by removing the leg cuticle and exposing the organs of the inner ear [7, 26]. This current available method has also been used with electrophysiology to measure the responses of sensory cells to sound-induced mechanical forces [25]. Yet this protocol might have negative effects in the natural operation of the ear. For example, draining the AV's fluid compromises the hydrostatic equilibrium of the system [6, 27]. On the other hand, some auditory processes in the inner ear of bush-crickets were

measured non-invasively using laser Doppler vibrometry (LDV) [6]. The authors speculated that this possible perhaps due to either translucent or thin ear cuticles, yet the mechanism by which this was possible is not understood [27]. Thus, understanding the properties of the ear cuticle is of fundamental importance for furthering research on measuring auditory activity using non-invasive techniques.

In this study, we quantified cuticle transparency across six species with different levels of cuticular pigmentation, and established the relationship between transparency, cuticle thickness, and LDV measurements of auditory activity. We hypothesise that transparency is the main cuticle property allowing the precise recording, and measurement of TWs and tonotopy in the inner ear of bush-crickets. Using the species with the highest cuticular transparency, the glass bush-cricket *Phlugis poecila*, we exemplify the retrieval of these complex auditory parameters from the inner ear, achieved non-invasively *in vivo*.

2. Materials and Methods

2.1. Specimens

Female and male adults of *Copiphora gorgonensis*, *C. vigorosa*, *Phlugis poecila*, *Neoconocephalus affinis*, *Nastonotus foreli*, and *Acantheremus* sp. were taken from colonies reared at the University of Lincoln, UK. Parental specimens were initially collected from two locations in the Colombian rain forest during December 2014 and November 2015. Collecting events took place at night (18:00 – 24:00) along established trails in the sampling areas, with a total of 48 hours of sampling activity. The sampling locations were El palmar de la Vizcaína and the National Natural Park, Gorgona. The former is an oil palm research centre surrounded by patches of tropical rain forest situated in the valley of the Magdalena river, 32 km from the municipality of Barrancabermeja, Santander (lat. 6°59'02.3"N; long 73°42'20.2"W). The latter is an island situated at 35 km from the Pacific coast of Colombia

(lat 2°47′ to 3°6′ N; long 78°6′, to 78°18′W). The park's ecosystem is classified as tropical wet forest with an area of 13.33 km^2. Collected specimens were transported to the University of Lincoln, UK, under collection and exportation permit No COR 5494-14 (issued by the Administrative Unit of National Natural Parks of Colombia).

2.2. Cuticle transparency measurements

Cuticle transparency was quantified by measuring the transmittance (ratio of the transmitted radiant flux to the incident radiant flux) of the cuticle covering the hearing organ. Cuticle samples were dissected from live specimens and placed in a cavity well microscope slide containing insect saline solution [28]. A 50 µm diameter optic fibre connected to a spectrophotometer (USB2000 Fibre Optic Spectrometer, Ocean optics Inc., Oxford, UK) was placed on the projector lens in the camera ocular of a compound light microscope. For all the measurements a 40X objective lens was used and the reference light was the illumination system of the microscope (Halogen lamp), with brightness maintained at 5 volts consistently for all experiments. The spectrophotometer detector unit was connected to a computer via an USB port and the collected measurements were transformed into digital format using the OOIBase32 spectrophotometer operating software (Ocean Optics Inc., Oxford, UK). The software calculates the percentage of energy passing through a sample relative to the amount that passes through the reference (equation 1).

$$\%T_\lambda = \frac{S_\lambda - D_\lambda}{R_\lambda - D_\lambda} \times 100\% \quad (1)$$

Where $\%T_\lambda$ is the percentage of transmittance at wavelength λ, S_λ is the sample intensity, D_λ is the dark intensity, R_λ is the reference intensity [29].

For each transmittance measurement a reference spectrum was taken with the light source on and a blank in the sampling region. The dark reference spectrum was taken with the light

path blocked, and a stray light correction was applied using boxcar pixel smoothing and signal averaging (10 averages).

2.3. Artificial actuator vibrations measured through transparent cuticle

A piece of freshly dissected cuticle from the dorsal ear area and a reference vibratory surface were used to evaluate the effects of the cuticle transparency on the laser Doppler vibrometry measurements, and to investigate whether the laser records ear vibrations on the cuticle, or on the CA through the cuticle. Ear top cuticles were dissected from one of the forelegs of live specimens from all species excluding *N. affinis* and fixed with a mixture of beeswax (Fisher Scientific, Bishop Meadow Road, Loughborough, UK) and colophonium (Sigma-Aldrich, Dorset, UK) to the tip of a copper rod (0.632 cm diameter and 23 cm long). Using a micromanipulator the external surface of sample was placed perpendicular between the laser head and the cone of a tweeter speaker enclosed in a custom made acoustic attenuating box (figure 2*a*). A 30 kHz pure tone was used as a reference signal and a 1/8" condenser microphone (Brüel & Kjaer, 4138-A-015 and preamplifier model 2670, Brüel & Kjaer, Nærum, Denmark) was positioned approximately 2-3 mm from the cuticle to monitor the acoustic isolation of the attenuating box and to ensure that the sound stimulus was not eliciting vibrations on the cuticle. The laser beam was focused on the cuticle and a digital scanning grid of approximately 450 points was set on the dorsal surface of the piece of cuticle. The recording time for each of the measuring points was 32 ms (5 averages), with a sampling rate of 512 kHz. The vibratory response was measured in displacement after applying a 1 kHz high-pass filter. As a control, the cuticle was removed and the surface of the speaker was scanned using the same settings and grid of points. The effect of the cuticle on the laser signal was estimated by calculating the ratio between the displacement response of the laser beam through the cuticle and the control surface.

2.4. Cuticle thickness

Cuticle thickness was measured to evaluate the effects of this property on the laser signal response. For this, the previously dissected cuticle samples were cut transversally lengthwise down the midpoint of the sample. Samples were then placed on an aluminium scanning electron microscope stub using a carbon tape. Digital images were captured and analysed with a FEI Inspect S50 microscope (FEI, Hillsboro, OR, USA). Measurements were made with the graphics software Coreldraw X7 (Corel corporation, Ottawa, Canada) using the dimension tool and adjusting the scale to real world values using the scale bar from each individual SEM image (electronic supplementary material, figure S1).

2.5. Mounting the specimens for LDV measurements of travelling waves

Protocols for measuring ear activity with LDV follows Montealegre-Z *et al*. [6]. For the LDV experiments, insects were initially anesthetized with a triethylamine-based mix (FlyNap®, Carolina Biological Supply Company, Burlington, North Carolina, USA) to facilitate the fastening to a horizontal brass platform (5 mm wide, 1 mm thick and 70 mm long). The dorsal pronotal area and legs, except for the frontal pair, were fixed to the platform using a mixture of beeswax (Fisher Scientific, Bishop Meadow Road, Loughborough, UK) and colophonium (Sigma-Aldrich, Dorset, UK). The front legs were restrained using brass wires, which allowed positioning of the tibia and femur in a 90 degrees angle. Additionally, the brass plate was attached to an articulated aluminium rod (150 mm long, 8 mm diameter) allowing the dorsal surface of the ear to be placed perpendicular to the scanner's laser beam. All experiments were carried out inside an acoustic booth, IAC Acoustics (Series 120a, internal length 2.40 m, width 1.8 m, and height 1.98 m), at room temperature (24–26°C) and relative humidity of 32-35%. The acoustic booth provides an internal reduction to external noise of at least 59 dB at 2 kHz and above (manufacturers information). The scanning head of the laser and the experimental setup were placed on Melles Griot Optical

Table Breadboard, Pneumatic Vibration Isolation (1m x 1m area) (Melles Griot, Rochester, NY).

2.6. LDV measurements of travelling waves

The sound-induced vibration pattern of the ear was measured using a micro-scanning laser Doppler vibrometer (Polytec PSV-500; Waldbronn, Germany) fitted with a close up attachment. The mounted specimens were positioned so that the cuticle overlaying the ear was perpendicular to the lens of the laser unit. A loudspeaker was positioned 30 cm, ipsilateral to the specimen to broadcast the sound stimulus (electronic supplementary material, figure S2). Periodic chirps were used as the acoustic stimulus, generated by the Polytec software (PSV 9.0.2), passed to an amplifier (A-400, Pioneer, Kawasaki, Japan), and sent to the loudspeaker (Ultrasonic Dynamic Speaker Vifa, Avisoft Bioacoustics, Glienicke, Germany). The periodic chirps contained frequencies between 5 and 80 kHz, and the stimulus was flattened so all frequencies were represented at 60 dB ±1.5 dB (SPL re 20 µPa) at the position of the ear. A 1/8" microphone (Brüel & Kjaer, 4138-A-015 and preamplifier model 2670, Brüel & Kjaer, Nærum, Denmark) was placed at the position of the ear to monitor and record the acoustic stimulus at the position of the ear as a reference (electronic supplementary material, figure S2). The laser system was used in scan mode. A grid of scan points on the dorsal surface of the CA was established using the PSV 9.2 acquisition software (Polytec, Waldbronn, Germany). Depending on the size of the insect's leg, the actual number of measuring points per grid varied among specimens, with ~800 points per ear. Within the frequency domain setting of the vibrometer, a frequency spectrum was calculated for each point using a FFT with a rectangular window, at a sampling rate of 256 kilo samples/second, 64 ms sampling time with a frequency resolution of 15.625 Hz. A high-pass filter of 1 kHz was applied to the both the vibrometer and reference microphone signals during the scanning process.

2.7. Data analysis

The relationship between laser response (a ratio), cuticular thickness (μm), and cuticular transmittance (%) were analysed using linear mixed effects (LMMs). Species was fitted as a random effect to account for species-differences in samples sizes. Parameters were logged before analysis. Models with and without interactions terms between cuticular thickness and cuticular transmittance were tested using likelihood ratio tests. The inclusion of the interaction significantly improved the model (χ^2_1=8.54, P<0.001). The relationship between cuticular thickness and transmittance was tested with a Pearson's correlation.

Data from all scanned points were examined using the PSV 9.2 presentation software (Polytec, Waldbronn, Germany). Frequency spectrums, ear displacement animations, and oscillation profiles were produced for selected frequencies within the recorded range. Frequency spectrums of the vibrometry data were normalised to those of the reference signal by computing the transfer function of the two [30]. For the TWs analysis, coordinates and displacement values from points corresponding to a 1 mm profile line set distal to proximal on the measured grid were exported as an ASCII file. The obtained data points were analysed using a custom Matlab code (Matworks Inc., Nauticks, USA), which generates plots of the TWs recorded from the scanned ears. The plots allowed us to visualise and measure the velocity response of each point in the frequency domain. The graphical representation was used to evaluate two of the TWs' criteria: asymmetric envelope and phase lag [30]. Furthermore, TWs' propagation velocity and wavelength were calculated from the phase response using equations 2-4.

$$\delta_t = \frac{\delta_\phi}{2\pi f} \quad (2)$$

$$V_{wave} = \frac{\delta_x}{\delta_t} \quad (3)$$

$$\lambda = \frac{2\pi\delta_x}{\delta_\phi} \quad (4)$$

Where *f* is wave frequency (Hz), δ_ϕ is phase difference (rad) between two points at different locations, δ_t is the travel time (s), δ_x is the distance travelled (m), V_{wave} is wave velocity and λ is wavelength [1, 30]. We then tested the relationship between these parameters and frequency using LMMs. In each model, individual katydid was fitted as a random effect. For all LMMs, degrees of freedom were calculated using Sattherwaite's approximation. Statistical analysis was carried out using the lme4 package [31] run in R version 3.3.1 [32]

3. Results

3.1. Cuticle transmittance

We quantified cuticle transparency across six species (figure 1*a*), and established the relationship between this property, cuticle thickness and LDV measurements of auditory activity. Using a spectrophotometer, cuticle transparency was quantified by measuring the transmittance (ratio of the transmitted radiant flux to the incident radiant flux) of the cuticle covering the hearing organ. Transmittance percentage values for all measured cuticles increased with wavelength in the visible light spectrum, 370-800 nm (figure 1*b*). At the light spectrum wavelength of the LDV laser (633 nm, Polytec PSV-500; Waldbronn, Germany) the curves can be distinguished into two groups. One group with transmission values relatively high, *P. poecila* and *C. gorgonensis* with averages of 73.73% ± 3.10 and 59.93% ± 4.15 respectively (mean ± SE, figure 1*c*). The second group includes values below 50% and it is formed by *C. vigorosa*, *Acantheremus* sp. *N. affinis*, and *N. foreli* with transmission percentages of 40.00% ± 3.24, 34.14 ± 12.24, 33.46% ± 2.32, and 18.82% ± 2.64 respectively (mean ± SE).

3.2. Laser Doppler vibrometry ratio response

The effect of cuticle transparency specifically in relation to transmission of light from a LDV was calculated as a ratio of the LDV response (measured as displacement) from a reference

vibrating surface (a membrane on a speaker playing a sine wave, figure 2*a*), and the same surface as measured through a sample of ear cuticle. The relationship between this LDV response and cuticle transmission, including cuticle thickness, was quantified through linear regression of these variables. Cuticle thickness was obtained by measuring cross sections of dissected ear cuticle (electronic supplementary material, figure S1). A linear mixed effect model found that laser displacement response ratio (L_r) was significantly related to the interaction between cuticle thickness and transmittance values (LMM: cuticular thickness x transmittance β±SE=0.90±0.31, $F_{1,18.07}$=8.53, P=0.009; LMM: cuticular thickness β±SE=-3.52±1.11, $F_{1,16.13}$=9.96, P=0.006; LMM: transmittance β±SE=4.08±1.30, $F_{1,18.07}$=9.82, P=0.006). Lowest laser displacement response ratio (L_r) occurred when both the cuticle was thin and when transmittance was low (figure 2*b*); the highest laser displacement response ratio (L_r) occurred when transmittance was high and cuticles were thinnest (*P. poecila:* mean±SE=-0.24±0.07). Transmittance and cuticle thickness were not correlated (r_p=-0.09, P=0.667).

3.3. *In vivo* measurement of travelling waves

In order to corroborate the feasibility of transparent species for *in vivo* audition experiments, the auditory activity of specimens of *P. poecila* was investigated as this species presented the highest transmittance values and thinnest cuticles. Non-invasive measurements of tonotopy and TWs *in vivo* were done by directly measuring the sound-induced vibration pattern of the ear using LDV (figure 3*a,* example of LDV output, figure 3*b*-*c*, see also electronic supplementary material, Movie S1). A spatially discrete response was observed for frequencies between ~10 and ~60 kHz from non-invasive measurements along the length of the hearing organ (figure 4*a*-*d*). With increasing stimulus frequency, the maximum response shifts towards the distal part of the leg (figure 4*a*-*d*) as predicted by the TW model of cochlea function.

The measured response in the inner ear satisfies two criteria for the inference of TWs: (i) asymmetric envelope and (ii) phase lag [1]. The magnitude of CA displacement shows an asymmetric envelope around the point of the maximal deflection. This point is also the location where the wave is seen to compress before dying off. TW asymmetry was evaluated as the response gain (mm/ s/ Pa) along a transect line across the CA for different frequencies (figure 4*e*-*g*) and it was observed that the position of the maximum displacement of the TW envelope varies with frequency. At 19 kHz the wave is asymmetrical about 720 µm along the transect (figure 4*e*), at 25 kHz the asymmetry occurs around 577 µm (figure 4*f*), and for 47 kHz the same phenomenon is observed approximately at 447 µm (figure 4*g*). Similarly, the phase response across the CA displays an increasing lag along the transect (figure 4*e*-*g*). The lag increases as a function of frequency; for instance, at 19 kHz the phase lag is 281°, while at 47 kHz the lag reaches 419° difference between the initial and final phase angle.

Velocity and wavelength of propagation are parameters of TW that can be acutely characterised with our approach. The velocity of the TW in the inner ear of *P. poecila* increased from 6.22±1.22 to 18.55±3.04 in a frequency range of 10 kHz to 50 kHz. The wavelength on the other hand decreased from 0.62±0.12 to 0.37±0.06 for the same frequency range. In our measurements, TW's velocity was significantly positively related to sound frequency (LMM: β±SE=0.31±0.02, $F_{1,103}$=315.60, P<0.001; figure 4*h*). Conversely, there was a significant decrease in wavelength size as frequency increased (LMM: β±SE=-0.006±0.001, $F_{1,103}$=77.48, P<0.001; figure 4*i*).

4. Discussion

We have confirmed cuticle transparency and cuticular thickness as primary factors allowing the non-invasive measurement of TWs and auditory mechanisms in the bush-cricket inner ear. Furthermore, our analysis reveals that transmittance of light through the cuticle is a reliable indicator of a species' suitability for experiments specifically using LDV. The lack of

correlation between cuticle transmittance and thickness indicates that pigmentation affects transparency, and in turn, laser measurements. This explains why established model species in insect hearing research like *Mecopoda elongata* [7] were not suitable in attempts of non-invasive laser measurements [27].

From the six species studied, *P. poecila* is a good model for auditory research due to its exceptional cuticle transparency and hearing capabilities. This could also apply to many species of the same subfamily (Meconematinae) within the genus *Phlugis* or related genera, which are also known as 'glass' or 'crystal bush-crickets' (or katydids). Males *P. poecila* produce calling songs to attract females using a broadband with a main carrier frequency peaking around 50 kHz (electronic supplementary material, figure S4). Our non-invasive approach shows that the ears of this species also incorporates a wide spectrum of frequencies from the audible to the ultrasonic range (at least 6-70 kHz, Fig. 4), and overlap the hearing ranges of humans and other vertebrates.

Several parameters of the auditory process could be measured non-invasively from the inner ear using LDV. Yet, to which extent some of the values recovered are real is unknown. Scattering of the laser beam at the cuticle (externally and internally) and at the AV might have an effect of the final values measured (for instance mechanical amplification). The presence of a liquid medium between the cuticle and the CA, reduces the laser beam scattering by providing a refractive index-matching effect [33]. The chemical composition of the AV fluid remains unknown, but it is likely that its refractive index, as reported for the haemolymph of other insects [34], is higher than that of the water (at 1.33). Therefore, due to a possible high refractive index, the AV fluid might increase the resolving power between the cuticle and the CA, as occurs with the use of immersion oils in light microscopy [35]. Finally, we think that the AV's geometry combined with the refractive index of the liquid together have an optical effect analogous to a plano-convex lens. As a consequence, this property increases the numerical aperture of the laser beam while reducing the characteristic irradiance loss of a Gaussian beam [36]. While refractive index of the AV fluid was not

measured in this study, future efforts should aim to account for this optical effect and to correct the LDV values of velocity/displacement accordingly [37, 38].

Taking advantage of the high level of cuticle transparency and wide frequency bandwidth of auditory perception (electronic supplementary material, figure S3) in *Phlugis* spp., we corroborated the use of bush-crickets as an alternative system for the non-invasive study of auditory processes. The observed phase lag and asymmetric envelope along the CA (figure 4*e*-*g*) allowed us to characterise the auditory response as a TW with displacement maxima at tonotopically specific locations. The obtained TW velocities and wavelengths are shown (figure 4*h* and 4*i*). These parameters have been calculated in the bush-cricket *Mecopoda elongata* by opening the cuticle and draining the natural AV fluid [12]. The data presented here was collected non-invasively from an intact system, reducing the effects of surgically opening the inner ear cavity (e.g. changes in the hydrostatic pressures and fluid density [6, 27]. It has been shown that the amplitude velocity of the CA decreases rapidly when the system is altered by, for example, draining its fluid, and that this operation causes also alters the phase of the tympana associated tympana [27]. However, the decrease in TW wavelength with increasing frequency, and the corresponding increase in TW velocity, presented here is in good agreement with predictions of TW function as observed in vertebrate [1, 39] and invertebrate [6, 7] models.

Understanding hearing processes such as tonotopy and TWs in mammals is crucial to further auditory research regarding nonlinear processes within the cochlea [13]. As mentioned before, anatomical limitations for accessing and obtaining data *in vivo*, and in an intact system, has been a major drawback in this field. Recently, methods for the measurement of auditory activity *in vivo* have improved notably for mammals. Developments with various techniques using optical coherence tomography (OCT), provides a visual technique for depth-resolved displacement measurements of TWs through the bony shell that protects the cochlea [12, 40]. Although such OCT techniques appear to be non-invasive, it still requires the middle ear bulla to be surgically treated to allow visual access to

the cochlea. This highlights the importance of developing novel and non-invasive techniques for the acquisition of TW data, as an important part of the complex auditory system. Attempts to relate the biomechanical tonotopy to the frequency tuning of the corresponding sensory cells in bush-crickets have produced important advances in this field [23], and the methodology presented here provides an opportunity for refinement of currently accepted experimental protocols. The reduced number of auditory sensory neurons, and the short length of the CA in theory compromises frequency resolution in the bush-cricket ear [7, 30, 42]. But certainly, these systems are not well understood and until the problem is rigorously approached, the phenomena of frequency resolution and sensitivity will remain elusive.

5. Conclusion

The transparent cuticle effectively supports the visualization and measurement of the auditory activity with no manipulation of the hearing organ required. The main advantage of this approach is that it overcomes the need for surgical intervention (i.e. removing the cuticle). Additionally, the ability to image through the cuticle provides the opportunity for experimental manipulation, such as the use of voltage-sensitive dyes to follow neuron activity in real time of the mechano-sensory cells involved in the hearing process [43-45]. Furthermore, from the point of view of invasive experimental protocols, invertebrates, and especially insects, are ideal substitutes within the 3Rs framework [46]. This work achieves not only *replacement*, by providing a possible alternative to vertebrate models, but also *refinement*, by using intact systems and noninvasive measurement, As animals are unharmed during measuring, this has the potential to also *reduce* animal usage.

The bush-cricket inner ear is functionally and structurally less complex, yet smaller than those of mammals. For instance, the number of mechano-sensory cells is considerably lower in bush-crickets. Even so, the physical principals underlying hearing in mammals are the same for hearing in bush-crickets [41]. The bush-cricket frequency analyser organ (the CA-AV) is uncoiled and the tonotopic organization takes place in a relatively short distance

(approximately one third of the length of the mammalian basilar membrane), and individual cap cells are visible on the surface of the tectorial membrane along the CA (figure S3). Such features provide unprecedented opportunity for experimental manipulation and, by the methodology presented here, for the collection of high-quality data. For example, a tentative application of such studies would be the investigation of an analogous mechanical origin of the TWs observed in the cochlea, and currently two hypotheses has been proposed to explain this phenomenon. Firstly, that TWs arise from anisotropic properties of the basilar membrane, resulting in tonotopically arranged displacement maxima causing excitation of the sensory cells [1]. And secondly, that the observed TW is a by-product of independently resonating sensory cells, coupled by a tectorial membrane [47]. We believe that this type of study, and novel experimental designs, may open avenues of research which help answer such fundamental questions in auditory mechanics, and could provide insights into the evolution of acoustic perception, the likes of which cannot be attained by only investigating mammalian models.

Authors' contributions. F.S-S. and F.M-Z., conceived and designed the experiments. F.S-S. and B.C. performed the experiments. F.S-S., and C.D.S. analysed data. C.D.S. designed all the statistical models. F.S-S., B.C. and F.M-Z. wrote the manuscript. All authors reviewed the manuscript.

Competing interests. The authors have declared that no competing interests exist.

Funding. This study comprises part of a PhD dissertation supported by the School of Life Sciences, University of Lincoln (COSREC-2014-02). FSS received travelling funds for fieldwork from Santander International Exchange Bursary. The authors are currently sponsored by the Leverhulme Trust (grant no. RPG-2014-284). National Geographic (National Geographic Explorer's grant RG120495 to F.M.-Z.).

Acknowledgements

The Colombian Ministry of Environment granted a permit for fieldwork at Gorgona National Park (decree DTS0-G-31 11/2007 and decree DTS0-G-090 14/08/2014). All applicable international, national and/or institutional guidelines for the care and use of animals were followed. We thank Dr. Tom Pike for providing equipment and technical advice on light transmittance measurements. Thanks go to Stephany Valdés for her assistance during the experiments and fieldwork. We are also grateful to the Palmar de la Vizcaina, Cenipalma research station, for facilitating our stay and collection in their area, especially to Carlos Andres Sendoya for helping during our fieldwork at night. This paper was improved thanks to the constructive comments of two anonymous reviewers.

References

1. Robles L, Ruggero MA. 2001 Mechanics of the mammalian cochlea. *Physiol. Rev.* **81**, 1305-1352.

2. Dallos P. 1992 The active cochlea. *J. Neurosci.* **2**, 4575-4585.

3. von Békésy G. 1960 *Experiments in hearing*. McGraw-Hill, New York, NY.

4. Hudspeth AJ. 2014 Integrating the active process of hair cells with cochlear function. *Nat Rev Neurosci* **15**, 600-614. (doi:10.1038/nrn3786).

5. Gummer AW, Smolders JW, Klinke R. 1987 Basilar membrane motion in the pigeon measured with the mössbauer technique. *Hear. Res.* **29**, 63-92.

6. Montealegre-Z F, Jonsson T, Robson-Brown KA, Postles M, Robert D. 2012 Convergent evolution between insect and mammalian audition. *Science* **338**, 968-971. (doi:10.1126/science.1225271)

7. Palghat Udayashankar A, Kössl M, Nowotny M. 2012 Tonotopically arranged traveling waves in the miniature hearing organ of bushcrickets. *Plos One* **7**, e31008. (doi:10.1371/journal.pone.0031008)

8. Hillery CM, Narins PM. 1984 Neurophysiological evidence for a traveling wave in the amphibian inner ear. *Science* **225**, 1037-1039. (doi:10.1126/science.6474164)

9. Smolders JWT, Klinke R. 1986 Synchronized responses of primary auditory fibre-populations in caiman crocodilus (l.) to single tones and clicks. *Hear. Res.* **24**, 89-103. (doi:10.1016/0378-5955(86)90052-3).

10. Young E. 2007 Physiological acoustics. In *Springer handbook of acoustics* (ed. T.D. Rossing). Springer, New York, NY. pp. 429-457.

11. Russell I, Nilsen K. 1997 The location of the cochlear amplifier: Spatial representation of a single tone on the guinea pig basilar membrane. *Proc. Natl. Acad. Sci. USA.* **94**, 2660-2664.

12. Lee HY, Raphael PD, Park J, Ellerbee AK, Applegate BE, Oghalai JS. 2015 Noninvasive in vivo imaging reveals differences between tectorial membrane and basilar membrane traveling waves in the mouse cochlea. *Proc. Natl. Acad. Sci. USA.* **112**, 3128-3133. (doi:10.1073/pnas.1500038112/-/DCSupplemental)

13. Elliott SJ, Shera CA. 2012 The cochlea as a smart structure. *Smart. Mater. Struct.* **21**, 064001

14. Lagarde MMM, Drexl M, Lukashkina VA, Lukashkin AN, Russell IJ. 2008 Outer hair cell somatic, not hair bundle, motility is the basis of the cochlear amplifier. *Nat. Neurosci.* **11**, 746-748. (doi:10.1038/nn.2129).

15. Gerhardt HC, Huber F. 2002 *Acoustic communication in insects and anurans. Common problems and diverse solutions*. The University of Chicago Press, Chicago, IL. pp. 9-47.

16. Greenfield MD. 2002 *Signalers and receivers: Mechanisms and evolution of arthropod communication*. Oxford University Press, Oxford, UK. pp 174-218.

17. Gwynne DT. 2001 *Katydids and bush-crickets: Reproductive behaviour and evolution of the tettigoniidae*. Cornell University Press, Ithaca, NY.

18 Bailey WJ. 1990 The ear of the bushcriket. In *The tettigoniidae. Biology, systematics and evolution* (eds. W.J. Bailey & D.C.F. Rentz). Crawford House Press, Bathurst, Australia. pp. 217-247

19. Hoy RR, Robert D. 1996 Tympanal hearing in insects. *Annu. Rev. Entomol.* **41**, 433-450. (doi:10.1146/annurev.ento.41.1.433).

20. Yack JE. 2004 The structure and function of auditory chordotonal organs in insects. *Microsc. Res. Tech.* **63**, 315-337. (doi:10.1002/jemt.20051).

21. Jonsson T, Montealegre-Z F, Soulsbury CD, Brown KAR & Robert D. 2016 Auditory mechanics in a bush-cricket: direct evidence of dual sound inputs in the pressure difference receiver. J. R. Soc. Interface **13**, 20160560. (doi: 10.1098/rsif.2016.0560)

22. Oldfield BP. 1982 Tonotopic organization of auditory receptors in tettigoniidae (orthoptera, ensifera). *J. Comp. Physiol.* **147**, 461-469. (doi:10.1007/BF00612011)

23. Römer H. 1983 Tonotopic organization of the auditory neuropile in the bushcricket tettigonia viridissima. *Nature* **306**,60-62. (doi:10.1038/306060a0)

24. Stolting H, Stumpner A. 1998 Tonotopic organization of auditory receptors of the bushcricket pholidoptera griseoaptera (tettigoniidae, decticinae). *Cell. Tissue. Res.* **294**, 377-386.

25. Hummel J, Schöneich S, Kössl M, Scherberich J, Hedwig B, Prinz S, Nowotny M. 2016 Gating of acoustic transducer channels is shaped by biomechanical filter processes. *J. Neurosci.* **36**, 2377-2382. (doi:10.1523/jneurosci.3948-15.2016).

26. Palghat Udayashankar A, Kössl M, Nowotny M. 2014 Lateralization of travelling wave response in the hearing organ of bushcrickets. *Plos One* **9**, e86090. (doi:10.1371/journal.pone.0086090)

27. Montealegre-Z F, Robert D. 2015 Biomechanics of hearing in katydids. *Journal Compa. Physiol. A.* **201**, 5-18. (doi:10.1007/s00359-014-0976-1).

28. Fielden, A. 1960 Transmission through the last abdominal ganglion of the dragonfly nymph Anax imperator. J. Exp. Biol. **37**, 832–844.

29. Ocean optics Inc. 2001 Usb2000 fiber optic spectrometer: Installation and operation manual *Ocean Optics Inc., Dunedin, FL, USA*.

30. Windmill JFC, Gopfert MC, Robert D. 2005 Tympanal travelling waves in migratory locusts. *J. Exp. Biol.* **208**, 157-168. (doi: 10.1242/jeb.01332)

31. Bates D, Mächler M, Bolker B, Walker S. 2014 Fitting linear mixed-effects models using lme4. *arXiv preprint arXiv:1406.5823*. (doi: 10.18637/jss.v067.i01)

32. R Development Core Team. 2016 R a language and environment for statistical computing. Vienna, Austria, R Foundation for Statistical Computing.

33. Vargas G, Chan EK, Barton JK, Rylander HG, Welch AJ. 1999 Use of an agent to reduce scattering in skin. *Lasers Surg. Med.* **24**, 133-141. (doi:10.1002/(SICI)1096-9101(1999)24:2<133::AID-LSM9>3.0.CO;2-X)

34. MIYAJIMA S. 1982 Refrctive index in hemolymph and gut juice of the silkworm infected with some viruses. *J. Sericult. Sci. Jpn*. **51**, 176-181. (doi: 10.11416/kontyushigen1930.51.176)

35. Cargille JJ. Immersion oil and the microscope (ed 2). New York Microscopial Society Yearbook, Cargille-Sacher Laboratories, Inc., 1985.

36. Martí Duocastella, C.F., Serra, P. & Diaspro, A. 2015 Sub-wavelength laser nanopatterning using droplet lenses. Sci. Rep. 5. (doi:10.1038/srep16199)

37. Marsili, R., Pizzoni, L. & Rossi, G. 2000 Vibration measurements of tools inside fluids by laser Doppler techniques: uncertainty analysis. Measurement. **27**, 111-120. (doi:10.1016/S0263-2241(99)00062-7)

38. Sapozhnikov, O., Morozov, A. & Cathignol, D. 2009 Acousto-optic interaction in laser vibrometry in a liquid. Acoust. Phys. **55**, 365-375. (doi:10.1134/S1063771009030129)

39. Şerbetçioğlu, M.B. & Parker, D.J. 1999 Measures of cochlear travelling wave delay in humans: I. Comparison of three techniques in subjects with normal hearing. Acta otolaryngol. **119**, 537-543. (doi:10.1080/00016489950180757)

40. Warren, R.L., Ramamoorthy, S., Ciganović, N., Zhang, Y., Wilson, T.M., Petrie, T., Wang, R.K., Jacques, S.L., Reichenbach, T. & Nuttall, A.L. 2016 Minimal basilar membrane motion in low-frequency hearing. P. oNatl. Acad. Sci. USA. **113**, E4304-E4310. (doi:10.1073/pnas.1606317113)

41. Hoy, R.R. 1998 Acute as a bug's ear: an informal discussion of hearing in insects. In Comparative hearing: insects. Springer, New York, NY. pp. 1-17.

42. Rhode, W.S. & Recio, A. 2000 Study of mechanical motions in the basal region of the chinchilla cochlea. J. Acoust. Soc. Am. **107**, 3317-3332. (doi:10.1121/1.429404).

43. Nikitin, E., Aseev, N. & Balaban, P. 2015 Improvements in the Optical Recording of Neuron Activity Using Voltage-Dependent Dyes. Neurosci. Behav. Physiol. **45**, 131-138. (doi: 10.1007/s11055-015-0050-7)

44. Baden, T. & Hedwig, B. 2010 Primary afferent depolarization and frequency processing in auditory afferents. J. Neurosci. **30**, 14862-14869. (doi: 10.1523/JNEUROSCI.2734-10.2010)

45. Isaacson, M.D. & Hedwig, B. 2017 Electrophoresis of polar fluorescent tracers through the nerve sheath labels neuronal populations for anatomical and functional imaging. Sci. Rep. 7. (doi: 10.1038/srep40433)

46. Guhad, F. 2005 Introduction to the 3Rs (refinement, reduction and replacement). Journal of the American Association for Laboratory Animal Science **44**, 58-59.

47. Bell, A. 2012 A resonance approach to cochlear mechanics. PloS one 7, e47918.

Ethics approval

College of Science Research Ethics Committee (COSREC), University of Lincoln granted permission to conduct this research under number COSREC-2014-02, and authorised the participation of all researchers involved in this project.

Data availability

Raw data for ear cuticle transparency (measured as transmittance), ear cuticle thickness, and measurement of travelling wave parameters (wavelength and velocity) have been stored in Dryad repository (DOI: doi:10.5061/dryad.cs4m9).

Figure captions

Figure 1. Study species and cuticle transmittance. (*a*) Species of bush-cricket (Tettigonidae) used for the transmittance measurements. Top row habitus of the species, bottom row close up view of the ear region showing the colour and level of cuticle pigmentation for each species. Red circle indicates position of ear in bush-crickets. (*b*) Cuticle transmittance values for all species studied. Transmittance curves (percentage of light diffused through the ear dorsal cuticle [see also figure 2*a*]) measured in the visible light spectrum (370-800 nm). (*c*) Mean transmittance values (± SE) of the ear dorsal cuticle of all species at the laser beam wavelength (633 nm).

Figure 2. Effect of cuticle transmission and thickness on LDV experiments. (*a*) Diagram of experimental protocol for obtaining laser displacement ratios from freshly dissected ear cuticle. See text for details. Image not to scale. (*b*) Relationship of cuticle transmittance, cuticle thickness and laser displacement ratio.

Figure 3. LDV experimental set-up and output. (*a*) Diagram of experimental protocol for non-invasive measurements of auditory function in bush-crickets using LDV. See text for details. Image not to scale. (*b*) Laser vibration map showing the distribution of areas of high vibration amplitude. Inset: ear area scanned during the LDV experiments. (*c*) 3D representation of the same data in *b* of a travelling wave at 10 kHz through phases of 45 degrees of the oscillation cycle.

Figure 4. Spatial frequency mapping and travelling waves in the inner ear of the glass bush-cricket *Phlugis poecila*. (*a*) Close up view of the left leg ear showing a three-point transect on between the anterior (ATM) and posterior tympanal membrane (PTM). The locations where the maximum velocity were recorded in the ear for 19 kHz, 25 kHz, and 47 kHz are represented by P1, P2, and P3 respectively. (*b*-*d*) Frequency response measured as velocity gain at locations P1-P3. (*e*-*g*) Envelope reconstruction along the transect in A for 19 kHz, 25 kHz, and 47 kHz. The deflection envelopes are constructed by displaying phase increments

of 10° in the full oscillation cycle. The red colour broken line represents the phase lag in degrees (red scale in the right) for the same frequencies and distance. (*h*) The velocity of the travelling wave in *P. poecila*. (*i*) Travelling-wave wavelength in *P. poecila*.

Supplementary material captions

Supplementary Figure 1. Examples of cuticle dissections for quantification of cuticle thickness. (*a*) Dorsal view of the ear, red line indicates location of cross section dissection. (*b*) *Copiphora vigarosa*. (*c*) *Copiphora gorgonensis*. (*d*) *Phlugis poecila*. (*e*) *Acantheremus* sp. (*f*) *Nastonotus foreli*.

Supplementary Figure 2. Experimental set-up for non-invasively measuring travelling waves in bush-crickets. See text for details. Inset: preparation of the mounted bush-cricket.

Supplementary Figure 3. Cuticle transparency in a glass bush-cricket *Phlugis* sp. (*a*) Lateral view of the femur, the acoustic trachea is clearly visible through the cuticle without manipulation of the animal. (*b*) Dorsal view of the hearing organ. The cap cells (scolopidia) are visible through the cuticle.

Supplementary Figure 4. Acoustic analysis of the call of the two species exhibiting more cuticle light transmittance. (*a-c*) *Phlugis poecila* and (*d-f*) *Copiphora gorgonensis*. (*a*) Typical presentation of the call. (*b*) A single phonatome (closing stroke of the wings) in detail. (*c*) Spectral analysis of the phonatome in (*b*). Wide bandwidth of prevalent frequencies are apparent in the call of *P. poecila*. (*d*) Typical presentation of the call. (*e*) A single phonatome (closing stroke of the wings) in detail. (*f*) Spectral analysis of the phonatome in (*e)*. Note higher tonal purity and harmonic content in the call of *C. gorgonensis*.

Supplementary Movie S1. A video of the laser Doppler response of the crista acustica to a 10 kHz pure tone sound stimulus at 60 dB SPL. The animation is the resulting interpolation

of the measured points of the scanning grid. In the dorsal and side view of the ear, the motion occurs in a distal to proximal direction (from the bottom to the top area of the video and from left to right).

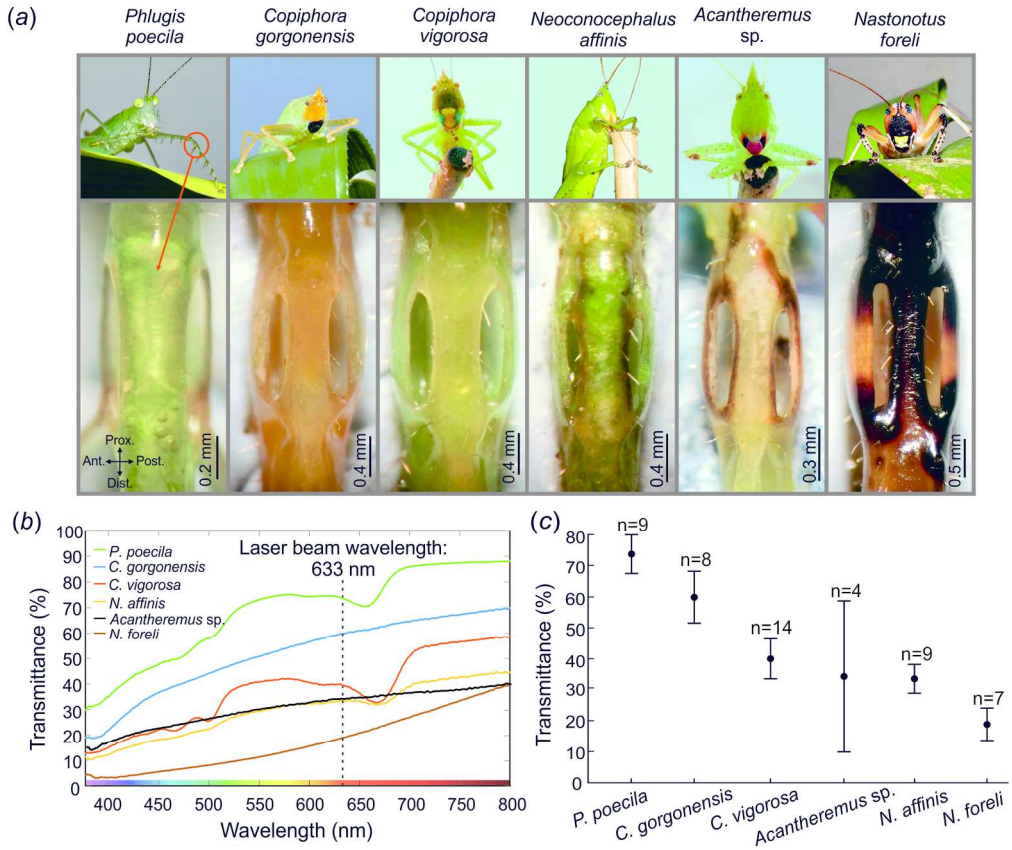

Figure 1. Study species and cuticle transmittance. (a) Species of bush-cricket (Tettigonidae) used for the transmittance measurements. Top row habitus of the species, bottom row close up view of the ear region showing the colour and level of cuticle pigmentation for each species. Red circle indicates position of ear in bush-crickets. (b) Cuticle transmittance values for all species studied. Transmittance curves (percentage of light diffused through the ear dorsal cuticle [see also figure 2a]) measured in the visible light spectrum (370-800 nm). (c) Mean transmittance values (± SE) of the ear dorsal cuticle of all species at the laser beam wavelength (633 nm).

176x148mm (300 x 300 DPI)

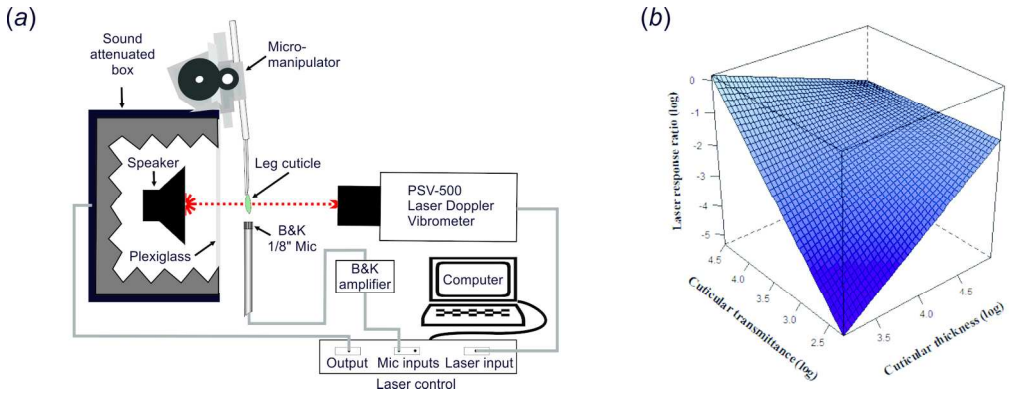

Figure 2. Effect of cuticle transmission and thickness on LDV experiments. (a) Diagram of experimental protocol for obtaining laser displacement ratios from freshly dissected ear cuticle. See text for details. Image not to scale. (b) Relationship of cuticle transmittance, cuticle thickness and laser displacement ratio.

170x65mm (300 x 300 DPI)

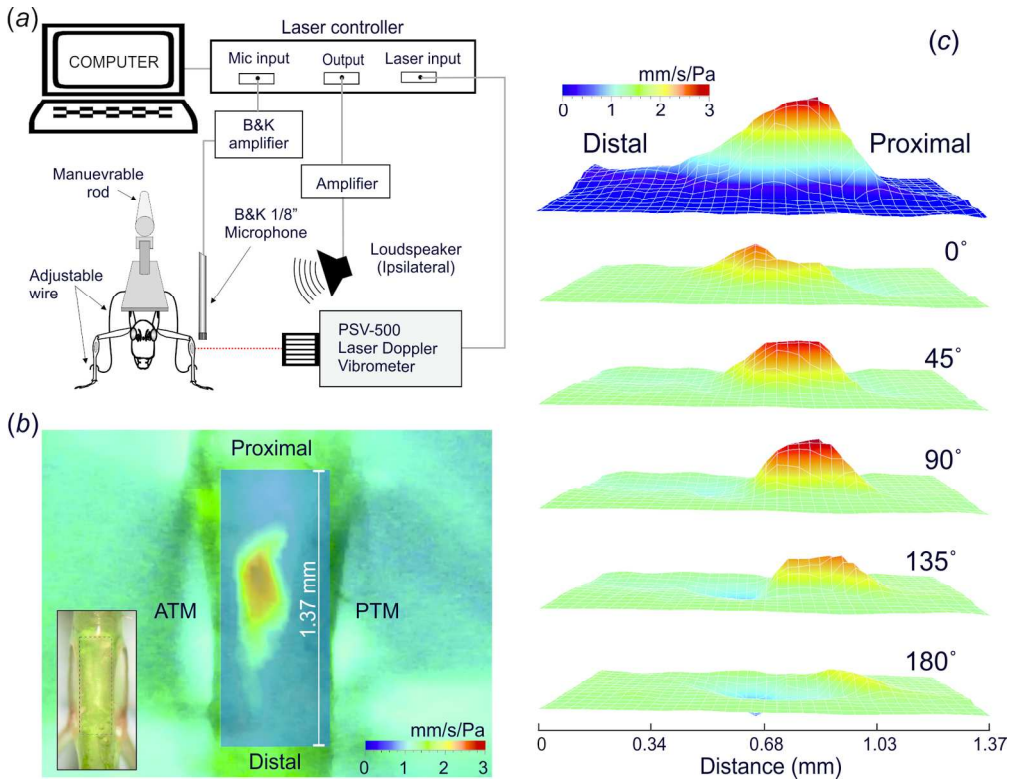

Figure 3. LDV experimental set-up and output. (a) Diagram of experimental protocol for non-invasive measurements of auditory function in bush-crickets using LDV. See text for details. Image not to scale. (b) Laser vibration map showing the distribution of areas of high vibration amplitude. Inset: ear area scanned during the LDV experiments. (c) 3D representation of the same data in b of a travelling wave at 10 kHz through phases of 45 degrees of the oscillation cycle.

Figure 4. Spatial frequency ma
162x124mm (300 x 300 DPI)

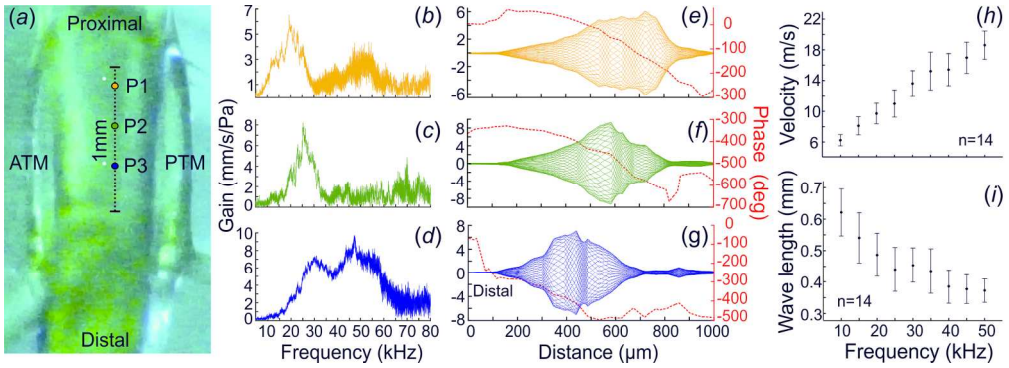

Figure 4. Spatial frequency mapping and travelling waves in the inner ear of the glass bush-cricket Phlugis poecila. (a) Close up view of the left leg ear showing a three-point transect on between the anterior (ATM) and posterior tympanal membrane (PTM). The locations where the maximum velocity were recorded in the ear for 19 kHz, 25 kHz, and 47 kHz are represented by P1, P2, and P3 respectively. (b-d) Frequency response measured as velocity gain at locations P1-P3. (e-g) Envelope reconstruction along the transect in A for 19 kHz, 25 kHz, and 47 kHz. The deflection envelopes are constructed by displaying phase increments of 10° in the full oscillation cycle. The red colour broken line represents the phase lag in degrees (red scale in the right) for the same frequencies and distance. (h) The velocity of the travelling wave in P. poecila. (i) Travelling-wave wavelength in P. poecila.

176x62mm (300 x 300 DPI)